

## BENCHMARK PROBLEMS IN STRUCTURAL CONTROL: PART I – ACTIVE MASS DRIVER SYSTEM

B.F. Spencer Jr.,<sup>1</sup> S.J. Dyke<sup>2</sup> and H.S. Deoskar<sup>3</sup>

### SUMMARY

This paper presents the overview and problem definition for a benchmark structural control problem. The structure considered — chosen because of the widespread interest in this class of systems (Soong 1990; Housner, *et al.* 1994b; Fujino, *et al.* 1996) — is a scale model of a three-story building employing an active mass driver. A model for this structural system, including the actuator and sensors, has been developed directly from experimentally obtained data and will form the basis for the benchmark study. Control constraints and evaluation criteria are presented for the design problem. A simulation program has been developed and made available to facilitate comparison of the efficiency and merit of various control strategies. A sample control design is given to illustrate some of the design challenges.

### INTRODUCTION

Tremendous progress has been made over the last two decades toward making active structural control a viable technology for enhancing structural functionality and safety against natural hazards such as strong earthquakes and high winds. The success of the First World Conference on Structural Control, held in Pasadena, California in August 1994, demonstrated the world-wide interest in structural control (Housner, *et al.* 1994a). The Conference attracted over 300 participants from 15 countries. The Second World Conference on Structural Control, to be held in Kyoto, Japan in the summer of 1998, promises to continue in this tradition.

Since the initial conceptual study by Yao (1972), many control algorithms and devices have been investigated, each with its own merits, depending on the particular application and desired effect. Clearly, the ability to make direct comparisons between systems employing these algorithms and devices is necessary to focus future efforts in the most promising directions and to effectively set performance goals and specifications. Indeed, the development of guidelines governing both performance and implementability is a meaningful and important task in itself.

This paper presents a benchmark structural control problem that can be used to evaluate the relative effectiveness and implementability of various structural control algorithms and to provide an analytical *testbed* for evaluation of control design issues such as model order reduction, spillover, control-structure interaction, limited control authority, sensor noise, available measurements, computational delay, *etc.* To achieve a high level of realism, an *evaluation* model is presented in the problem definition which is derived directly from experimental data obtained at the Structural Dynamics and Control/Earthquake Engineering Laboratory (SDC/EEL) at the University of Notre Dame. This model accurately represents the behavior of the laboratory structure and fully incorporates actuator/sensor dynamics. Herein, the evaluation model will be considered

---

1. Prof., Dept. of Civil Engrg. and Geo. Sci., Univ. of Notre Dame, Notre Dame, IN 46556-0767.

2. Assist. Prof., Dept. of Civil Engrg., Washington Univ., St. Louis, MO 63130-4899.

3. Former Grad. Assist., Dept. of Civil Engrg. and Geo. Sci., Univ. of Notre Dame, Notre Dame, IN 46556-0767.

as the real structural system. In general, controllers that are successfully implemented on the evaluation model can be expected to perform similarly in the laboratory setting. Several evaluation criteria are given, along with the associated control design constraints. A sample control design is presented to illustrate some of the design challenges. This benchmark problem can be viewed as an initial step toward development of standardized performance evaluation procedures.

## EXPERIMENTAL STRUCTURE

The structure on which the evaluation model is based is an actively controlled, three-story, single-bay, model building considered in Dyke, *et al.* (1994a, 1996a). The test structure, shown in Figs. 1 and 2, is designed to be a scale model of the prototype building discussed in Chung, *et al.* (1989) and is subject to one-dimensional ground motion. The building frame is constructed of steel, with a height of 158 cm. The floor masses of the model totaled 227 kg, distributed evenly between the three floors. The structural frame mass was 77 kg. The time scale factor is 0.2, making the natural frequencies of the model approximately five times those of the prototype. The first three modes of the model structural system are at 5.81 Hz, 17.68 Hz and 28.53 Hz, with associated damping ratios given, respectively, by 0.33%, 0.23%, and 0.30%. The ratio of model quantities to those corresponding to the prototype structure are: force = 1:60, mass = 1:206, time = 1:5, displacement = 4:29 and acceleration = 7:2.

For control purposes, a simple implementation of an active mass driver (AMD) was placed on the third floor of the structure. The AMD consists of a single hydraulic actuator with steel masses attached to the ends of the piston rod (see Fig. 3). The servo-actuated hydraulic cylinder has a 3.8 cm diameter and a 30.5 cm stroke. For this experiment, the moving mass for the AMD was 5.2 kg, and consisted of the piston, piston rod, and steel disks bolted to the end of the piston rod. The total mass of the structure, including the frame and the AMD, was 309 kg. Thus, the moving mass of the AMD is 1.7% of the total mass of the structure. Because hydraulic actuators are inherently open loop unstable, position feedback was employed to stabilize the control actuator. The position of the actuator was obtained using an LVDT (linear variable differential transformer), rigidly mounted between the end of the piston rod and the third floor.

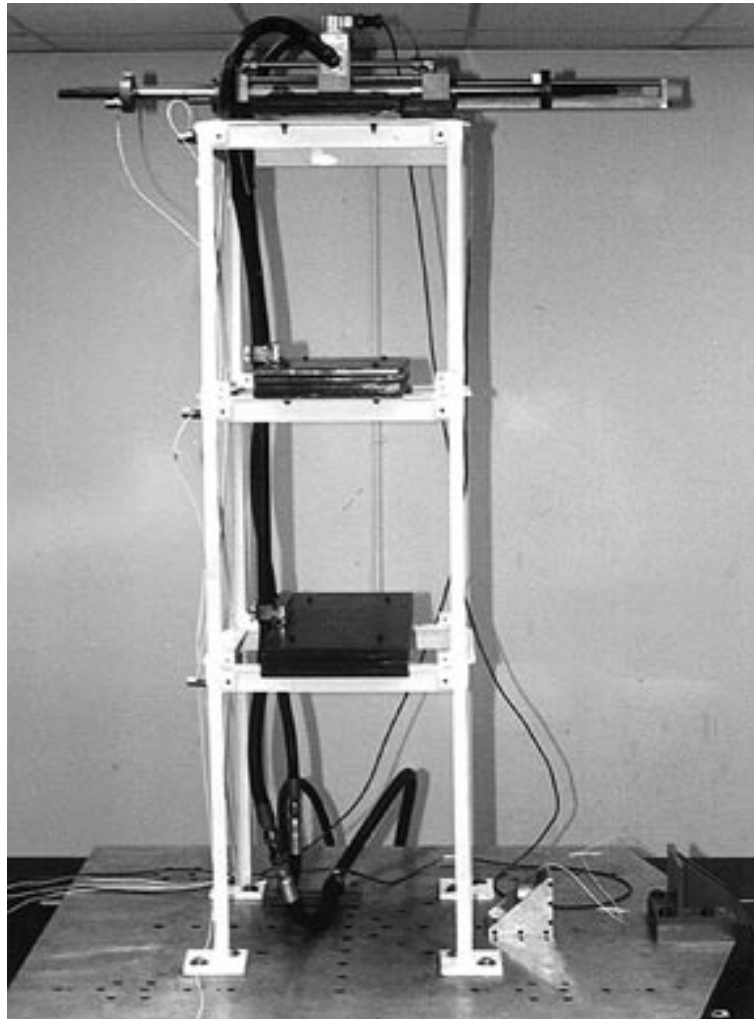


**Figure 1. Three Degree-of-Freedom Test Structure with AMD System.**

Structural displacements and velocities are difficult to obtain directly in full scale structures, because they must be measured relative to an inertial reference frame. Alternatively, acceleration measurements can readily be acquired at arbitrary locations on the structure. For this experiment, accelerometers were positioned on the ground, on each floor of the structure, and on the AMD, as shown in Fig. 2. The displacement of the AMD relative to the third floor was also measured using the LVDT mentioned above. Thus, the measurements that are directly available for control force determination are the three floor acceleration measurements, the ground acceleration, and the displacement and acceleration of the AMD (see Fig. 2). Additionally, pseudo absolute velocities are available by passing the measured accelerations through a second order filter that is essentially a high-pass filter in series with an integrator (Ivers and Miller, 1991).

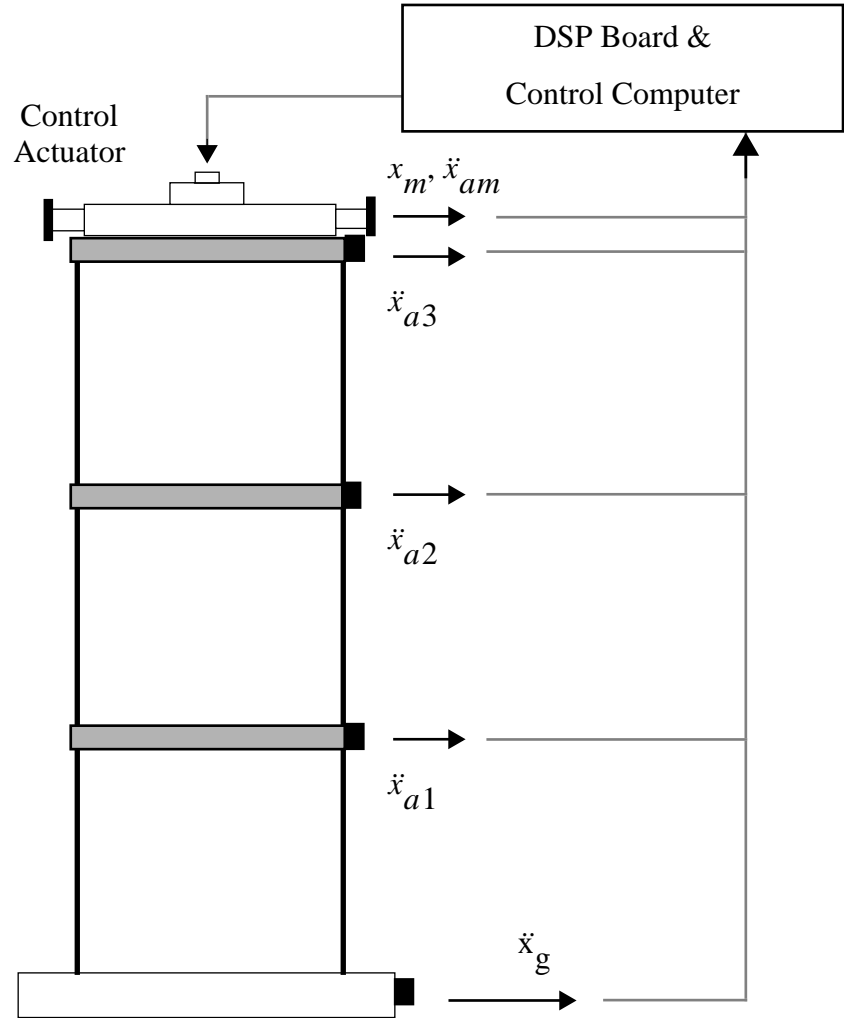


Figure 2. Schematic Diagram of Experimental Setup.

## EVALUATION MODEL

A high-fidelity, linear time-invariant state space representation of the input-output model for the structure described in the previous section has been developed. The model has 28 states and is of the form

$$\dot{\mathbf{x}} = \mathbf{A}\mathbf{x} + \mathbf{B}u + \mathbf{E}\ddot{x}_g \quad (1)$$

$$\mathbf{y} = \mathbf{C}_y\mathbf{x} + \mathbf{D}_yu + \mathbf{F}_y\ddot{x}_g + \mathbf{v} \quad (2)$$

$$\mathbf{z} = \mathbf{C}_z\mathbf{x} + \mathbf{D}_zu + \mathbf{F}_z\ddot{x}_g \quad (3)$$

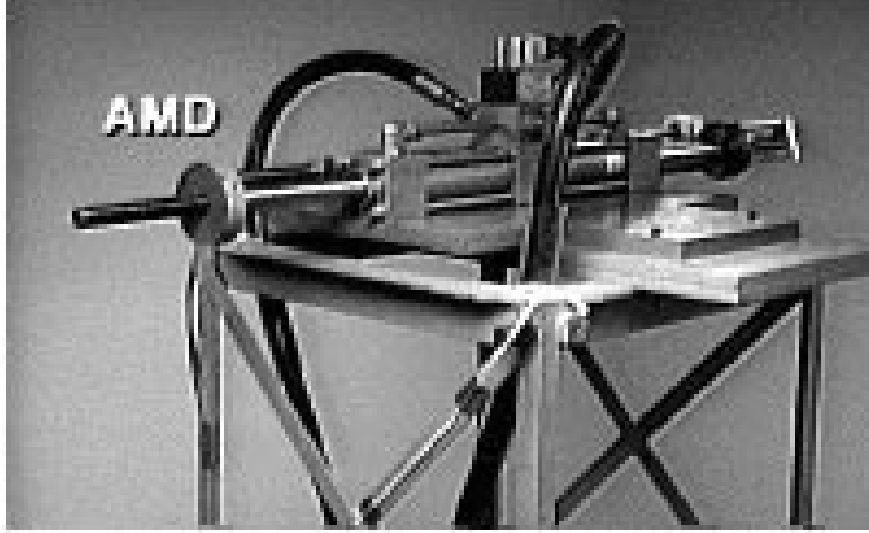


Figure 3. Active Mass Driver.

where  $\mathbf{x}$  is the state vector,  $\ddot{x}_g$  is the scalar ground acceleration,  $u$  is the scalar control input,  $\mathbf{y} = [x_m, \ddot{x}_{a1}, \ddot{x}_{a2}, \ddot{x}_{a3}, \ddot{x}_{am}, \ddot{x}_g]'$  is the vector of responses that can be directly measured,  $\mathbf{z} = [x_1, x_2, x_3, x_m, \dot{x}_1, \dot{x}_2, \dot{x}_3, \dot{x}_m, \ddot{x}_{a1}, \ddot{x}_{a2}, \ddot{x}_{a3}, \ddot{x}_{am}]'$  is the vector of responses that can be regulated. Here,  $x_i$  is the displacement of the  $i$ th floor relative to the ground,  $x_m$  is the displacement of the AMD relative to the third floor,  $\ddot{x}_{ai}$  is the absolute acceleration of the  $i$ th floor,  $\ddot{x}_{am}$  is the absolute acceleration of the AMD mass,  $\mathbf{v}$  is the vector of measurement noises, and  $\mathbf{A}$ ,  $\mathbf{B}$ ,  $\mathbf{E}$ ,  $\mathbf{C}_y$ ,  $\mathbf{D}_y$ ,  $\mathbf{C}_z$ ,  $\mathbf{D}_z$ ,  $\mathbf{F}_y$ , and  $\mathbf{F}_z$  are matrices of appropriate dimension. The coefficient matrices in Eqs. (1–3) are determined from the data collected at the SDC/EEL using the identification methods presented in Dyke, *et al.* (1994a,b, 1996a,b). The resulting model represents the input-output behavior of the structural system up to 100 Hz and includes the effects of actuator/sensor dynamics and control-structure interaction. Figure 4 provides a representative comparison between the model from Eqs. (1–3) and the experimental data. Note that the experimental data was obtained using a 16-bit data acquisition board. Thus, the difference between the experimental data and the model in Fig. 4a at low frequencies is due to the finite precision of the data acquisition system.

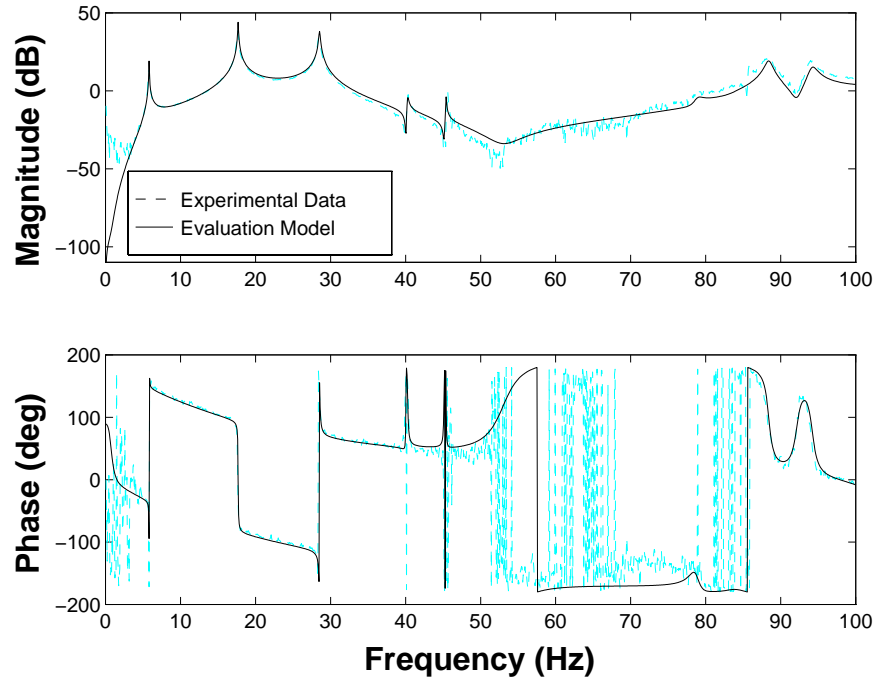
The model given in Eqs. (1–3) is termed the *evaluation* model and will be used to assess the performance of candidate controllers; that is, the evaluation model is considered herein to be the true representation of the structural system.

## CONTROL DESIGN PROBLEM

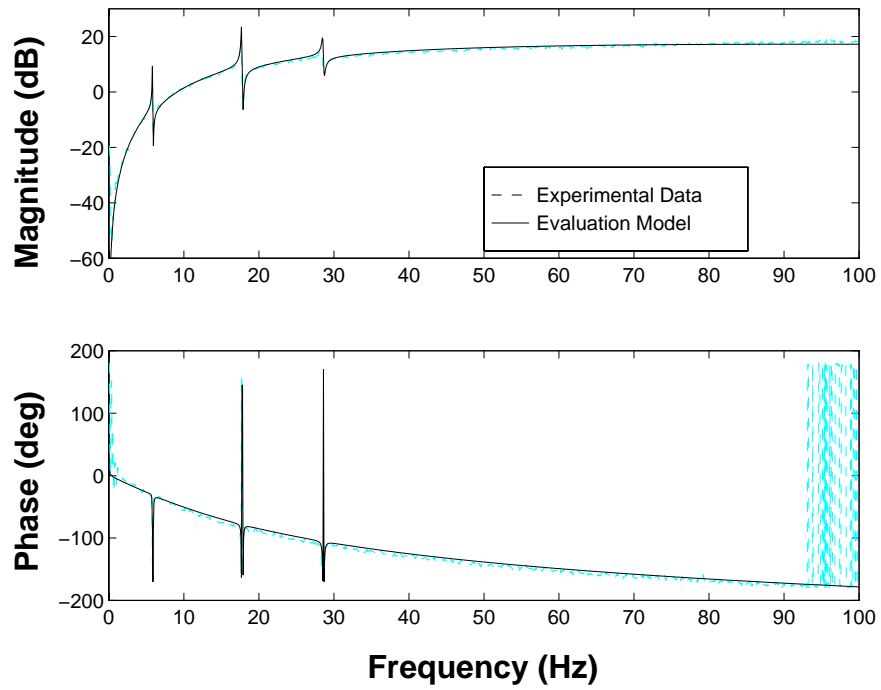
The control design problem is to determine a discrete-time, feedback compensator of the form

$$\mathbf{x}_{k+1}^c = f_1(\mathbf{x}_k^c, \mathbf{y}_k, u_k, k) \quad (4)$$

$$u_k = f_2(\mathbf{x}_k^c, \mathbf{y}_k, k) \quad (5)$$



(a)



(b)

**Figure 4. Representative Comparison of the Transfer Functions for the Test Structure and the Evaluation Model. (a) Actuator Command to 1st Floor Absolute Acceleration, (b) Actuator Command to AMD Absolute Acceleration.**

where  $\mathbf{x}_k^c$ ,  $\mathbf{y}_k$  and  $u_k$  are the state vector for the compensator, the output vector and the control command, respectively, at time  $t = kT$ . For this problem the performance of all control designs must be assessed using the evaluation model described previously. For each proposed control design, performance and stability robustness should be discussed. As detailed in the following paragraphs, the merit of a controller will be based on criteria given in terms of both rms and peak response quantities. Normally, smaller values of the evaluation criteria indicate superior performance.

#### *Evaluation Criteria: RMS Responses*

Assume that the input excitation  $\ddot{x}_g$  is a stationary random process with a spectral density defined by the Kanai-Tajimi spectrum

$$S_{\ddot{x}_g \ddot{x}_g}(\omega) = \frac{S_0(4\zeta_g^2 \omega_g^2 \omega^2 + \omega_g^4)}{(\omega^2 - \omega_g^2)^2 + 4\zeta_g^2 \omega_g^2 \omega^2} \quad (6)$$

where  $\omega_g$  and  $\zeta_g$  are unknown, but assumed to lie in the following ranges:  $20 \text{ rad/sec} \leq \omega_g \leq 120 \text{ rad/sec}$ ,  $0.3 \leq \zeta_g \leq 0.75$ . To have a basis for comparison, the spectral intensity is chosen such that the rms value of the ground motion takes a constant value of  $\sigma_{\ddot{x}_g} = 0.12 \text{ g's}$ , i.e.,

$$S_0 = \frac{0.03\zeta_g}{\pi\omega_g(4\zeta_g^2 + 1)} \text{ g}^2 \cdot \text{sec} \quad (7)$$

The first criterion on which controllers will be evaluated is based on their ability to minimize the maximum rms interstory drift due to all admissible ground motions. Therefore, the non-dimensionalized measure of performance is given by

$$J_1 = \max_{\omega_g, \zeta_g} \left\{ \frac{\sigma_{d_1}}{\sigma_{x_{30}}}, \frac{\sigma_{d_2}}{\sigma_{x_{30}}}, \frac{\sigma_{d_3}}{\sigma_{x_{30}}} \right\} \quad (8)$$

where  $\sigma_{d_i}$  is the stationary rms interstory drift for the  $i$ th floor, and  $\sigma_{x_{30}} = 1.31 \text{ cm}$  is the worst-case stationary rms displacement of the third floor of the uncontrolled building over the class of excitations considered (occurring when  $\omega_g = 37.3 \text{ rad/sec}$ ,  $\zeta_g = 0.3$ ). The interstory drifts are given respectively by  $d_1(t) = x_1(t)$ ,  $d_2(t) = x_2(t) - x_1(t)$  and  $d_3(t) = x_3(t) - x_2(t)$ .

A second evaluation criterion is given in terms of the maximum rms absolute acceleration, yielding a performance measure given by

$$J_2 = \max_{\omega_g, \zeta_g} \left\{ \frac{\sigma_{\ddot{x}_{a1}}}{\sigma_{\ddot{x}_{a30}}}, \frac{\sigma_{\ddot{x}_{a2}}}{\sigma_{\ddot{x}_{a30}}}, \frac{\sigma_{\ddot{x}_{a3}}}{\sigma_{\ddot{x}_{a30}}} \right\} \quad (9)$$

where  $\sigma_{\ddot{x}_{ai}}$  is the stationary rms acceleration for the  $i$ th floor, and  $\sigma_{\ddot{x}_{a30}} = 1.79 \text{ g's}$  is the worst-case stationary rms acceleration of the third floor of the uncontrolled building (occurring when  $\omega_g = 37.3 \text{ rad/sec}$ ,  $\zeta_g = 0.3$ ).

The hard constraints for the control effort are given by  $\sigma_u \leq 1$  volt,  $\sigma_{\ddot{x}_{am}} \leq 2$  g's and  $\sigma_{x_m} \leq 3$  cm. Additionally, candidate controllers are to be evaluated based on the required control resources. Three quantities,  $\sigma_{x_m}$ ,  $\sigma_{\dot{x}_m}$  and  $\sigma_{\ddot{x}_{am}}$ , should be examined to make the assessment. The rms actuator displacement,  $\sigma_{x_m}$ , provides a measure of the required physical size of the device. The rms actuator velocity,  $\sigma_{\dot{x}_m}$ , provides a measure of the control power required. The rms absolute acceleration  $\sigma_{\ddot{x}_{am}}$  provides a measure of the magnitude of the forces that the actuator must generate to execute the commanded control action. Therefore, the nondimensionalized control resource evaluation criteria are

$$J_3 = \max_{\omega_g, \zeta_g} \left\{ \frac{\sigma_{x_m}}{\sigma_{x_{30}}} \right\} \quad (10)$$

$$J_4 = \max_{\omega_g, \zeta_g} \left\{ \frac{\sigma_{\dot{x}_m}}{\sigma_{\dot{x}_{30}}} \right\} \quad (11)$$

$$J_5 = \max_{\omega_g, \zeta_g} \left\{ \frac{\sigma_{\ddot{x}_{am}}}{\sigma_{\ddot{x}_{a30}}} \right\} \quad (12)$$

where  $\sigma_{\dot{x}_{30}} = 47.9$  cm/sec is the worst-case stationary rms velocity of the third floor relative to the ground for the uncontrolled structure (occurring when  $\omega_g = 37.3$  rad/sec,  $\zeta_g = 0.3$ ).

#### *Evaluation Criteria: Peak Responses*

Here, the input excitation  $\ddot{x}_g$  is assumed to be a historical earthquake record. Both the 1940 El Centro NS record and the NS record for the 1968 Hachinohe earthquake should be considered. Because the system under consideration is a scale model, the time scale should be increased by a factor of 5 (*i.e.*, the earthquakes occur in 1/5 the recorded time). The required scaling of the magnitude of the ground acceleration is 3.5. The evaluation criterion is based on minimization of the nondimensionalized peak interstory drifts due to both earthquake records. For each earthquake, the maximum drifts are nondimensionalized with respect to the uncontrolled peak third floor displacement, denoted  $x_{30}$ , relative to the ground. Therefore, the performance measure is given by

$$J_6 = \max_{\substack{\text{El Centro} \\ \text{Hachinohe}}} \left[ \max_t \left\{ \frac{|d_1(t)|}{x_{30}}, \frac{|d_2(t)|}{x_{30}}, \frac{|d_3(t)|}{x_{30}} \right\} \right] \quad (13)$$

A second performance evaluation criterion is given in terms of the peak acceleration, yielding

$$J_7 = \max_{\substack{\text{El Centro} \\ \text{Hachinohe}}} \left[ \max_t \left\{ \frac{|\ddot{x}_{a1}(t)|}{\ddot{x}_{a30}}, \frac{|\ddot{x}_{a2}(t)|}{\ddot{x}_{a30}}, \frac{|\ddot{x}_{a3}(t)|}{\ddot{x}_{a30}} \right\} \right] \quad (14)$$

where the accelerations are nondimensionalized by the peak uncontrolled third floor acceleration, denoted  $\ddot{x}_{a30}$ , corresponding respectively to each earthquake.

The control constraints are  $\max_t |u(t)| \leq 3$  volts,  $\max_t |x_m(t)| \leq 9$  cm,  $\max_t |\ddot{x}_{am}(t)| \leq 6$  g's, and both the El Centro and the Hachinohe earthquakes should again be considered. Additionally, the candidate controllers are to be evaluated in terms of the required control resources as follows

$$J_8 = \max_{\substack{\text{El Centro} \\ \text{Hachinohe}}} \left[ \max_t \frac{|x_m(t)|}{x_{30}} \right] \quad (15)$$

$$J_9 = \max_{\substack{\text{El Centro} \\ \text{Hachinohe}}} \left[ \max_t \frac{|\dot{x}_m(t)|}{\dot{x}_{30}} \right] \quad (16)$$

$$J_{10} = \max_{\substack{\text{El Centro} \\ \text{Hachinohe}}} \left[ \max_t \frac{|\ddot{x}_{am}(t)|}{\ddot{x}_{a30}} \right] \quad (17)$$

where  $\dot{x}_{30}$  is the peak uncontrolled third floor relative velocity corresponding respectively to each earthquake.

For the El Centro earthquake,  $x_{30} = 3.37$  cm,  $\dot{x}_{30} = 131$  cm/sec and  $\ddot{x}_{a30} = 5.05$  g's. For the Hachinohe earthquake,  $x_{30} = 1.66$  cm,  $\dot{x}_{30} = 58.3$  cm/sec and  $\ddot{x}_{a30} = 2.58$  g's.

## CONTROL IMPLEMENTATION CONSTRAINTS

To make the benchmark problem as realistic as possible, the following implementation constraints are placed on the system:

1. As indicated previously, the measurements that are directly available for use in determination of the control action are  $\mathbf{y} = [x_m, \ddot{x}_{a1}, \ddot{x}_{a2}, \ddot{x}_{a3}, \ddot{x}_{am}, \ddot{x}_g]'$ . Although absolute velocities are not available, they can be closely approximated by passing the measured accelerations through a second order filter with the following transfer function

$$H_{\dot{x}\ddot{x}}(s) = \frac{39.5s}{39.5s^2 + 8.89s + 1} \quad (18)$$

where  $\dot{x}$  is the pseudo velocity response in that it will track the absolute velocity response above 1 Hz. Therefore, the pseudo velocities,  $\dot{x}_{a1}, \dot{x}_{a2}, \dot{x}_{a3}, \dot{x}_{am}, \dot{x}_g$ , are also available for determination of the control action, and the combined output vector is given by  $\mathbf{y} = [x_m, \ddot{x}_{a1}, \ddot{x}_{a2}, \ddot{x}_{a3}, \ddot{x}_{am}, \ddot{x}_g, \dot{x}_{a1}, \dot{x}_{a2}, \dot{x}_{a3}, \dot{x}_{am}, \dot{x}_g]'$ . For more information regarding practical issues associated with implementing the filter in Eq. (18), see Ivers and Miller (1991).

2. The controller for the structure is digitally implemented with a sampling time of  $T = 0.001$  sec.
3. A computation delay of 200  $\mu$  sec is required to perform the D-matrix calculations in the control action determination and for the associated A/D and D/A conversions (Quast, et al., 1995).
4. The A/D and D/A converters on the digital controller have 12-bit precision and a span of  $\pm 3$  V.



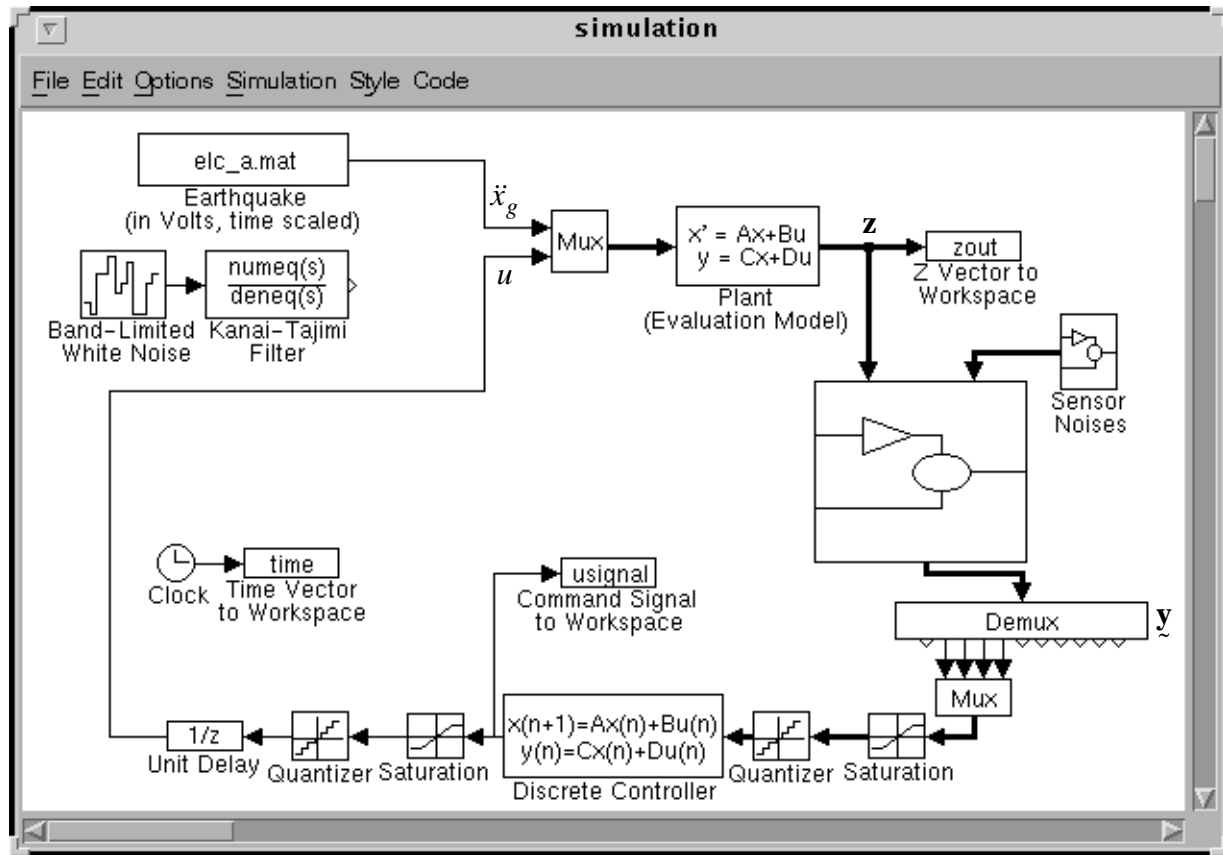


**Figure 5. SIMULINK Model for the Benchmark Problem.**

5. Each of the measured responses contains an rms noise of 0.01 Volts, which is approximately 0.3% of the full span of the A/D converters. The measurement noises are modeled as Gaussian rectangular pulse processes with a pulse width of 0.001 seconds.
6. To account for limited computational resources in the digital controller, the controller given in Eqs. (4) and (5) is restricted to have no more than 12 states.
7. The performance of each control design should be evaluated using the 28 state evaluation model given in Eqs. (1)–(3).
8. The controller given in Eqs. (4) and (5) is required to be stable.

The SIMULINK (1994) model shown in Fig. 5 has been developed to simulate the features and limitations of this structural control problem. Note that, although the controller is digital, the structure is still modeled as a continuous system. To reduce integration errors, a time step of 0.0001 sec is used in the simulation.

## SAMPLE CONTROL DESIGN

To illustrate some of the constraints and challenges of this benchmark problem, a sample linear quadratic Gaussian (LQG) control design is presented. The first step in this process is to de-

velop a reduced order model, designated the *design* model, for purposes of control design. The design model has the form

$$\dot{\mathbf{x}}_r = \mathbf{A}_r \mathbf{x}_r + \mathbf{B}_r u + \mathbf{E}_r \ddot{x}_g \quad (19)$$

$$\mathbf{y}_r = \mathbf{C}_{yr} \mathbf{x}_r + \mathbf{D}_{yr} u + \mathbf{F}_{yr} \ddot{x}_g + \mathbf{v}_r \quad (20)$$

where  $\mathbf{x}_r$  is a 10-dimensional state vector,  $\mathbf{y}_r = [\ddot{x}_{a1}, \ddot{x}_{a2}, \ddot{x}_{a3}, \ddot{x}_{am}]'$  and  $\mathbf{A}_r, \mathbf{B}_r, \mathbf{E}_r, \mathbf{C}_{yr}, \mathbf{D}_{yr}$  and  $\mathbf{F}_{yr}$  are the reduced order coefficient matrices. This design will not make use of the measurement of the ground excitation, the pseudo absolute velocities or the actuator displacement, although these measurements are available.

To simplify design of the controller,  $\ddot{x}_g$  is taken to be a stationary white noise, and an infinite horizon performance index is chosen that weights the accelerations of the three floors, *i.e.*,

$$J = \lim_{\tau \rightarrow \infty} \frac{1}{\tau} E \left[ \int_0^\tau \{ (\mathbf{C}_{yr} \mathbf{x}_r + \mathbf{D}_{yr} u)' \mathbf{Q} (\mathbf{C}_{yr} \mathbf{x}_r + \mathbf{D}_{yr} u) + r u^2 \} dt \right] \quad (21)$$

where  $r = 50$ , and all of the elements of the weighting matrix  $\mathbf{Q}$  are zero, except for  $Q_{11} = Q_{22} = Q_{33} = 1$ . Further, the measurement noise is assumed to be identically distributed, statistically independent Gaussian white noise processes, and  $S_{\ddot{x}_g \ddot{x}_g} / S_{v_i v_i} = \gamma = 25$ .

The separation principle allows the control and estimation problems to be considered separately, yielding a controller of the form (Stengel 1986; Skelton 1988)

$$u = -\mathbf{K} \hat{\mathbf{x}}_r \quad (22)$$

where  $\hat{\mathbf{x}}_r$  is the Kalman Filter estimate of the state vector based on the reduced order model. By the certainty equivalence principle (Stengel 1986; Skelton 1988),  $\mathbf{K}$  is the full state feedback gain matrix for the deterministic regulator problem given by

$$\mathbf{K} = (\tilde{\mathbf{N}}' + \mathbf{B}_r' \mathbf{P}) / \tilde{r} \quad (23)$$

where  $\mathbf{P}$  is the solution of the algebraic Riccati equation given by

$$\mathbf{0} = \mathbf{P} \tilde{\mathbf{A}} + \tilde{\mathbf{A}}' \mathbf{P} - \mathbf{P} \mathbf{B}_r \mathbf{B}_r' \mathbf{P} / \tilde{r} + \tilde{\mathbf{Q}} \quad (24)$$

and

$$\tilde{\mathbf{Q}} = \mathbf{C}_{yr}' \mathbf{Q} \mathbf{C}_{yr} - \tilde{\mathbf{N}} \tilde{\mathbf{N}}' / \tilde{r} \quad (25)$$

$$\tilde{\mathbf{N}} = \mathbf{C}_{yr}' \mathbf{Q} \mathbf{D}_{yr} \quad (26)$$

$$\tilde{r} = r + \mathbf{D}_{yr}' \mathbf{Q} \mathbf{D}_{yr} \quad (27)$$

$$\tilde{\mathbf{A}} = \mathbf{A}_r - \mathbf{B}_r \tilde{\mathbf{N}}' / \tilde{r} \quad (28)$$

Calculations to determine  $\mathbf{K}$  were done using the MATLAB (1994) routine *lqry.m* within the control toolbox.

The Kalman Filter optimal estimator is given by

$$\dot{\hat{\mathbf{x}}}_r = \mathbf{A}_r \hat{\mathbf{x}}_r + \mathbf{B}_r u + \mathbf{L}(\mathbf{y} - \mathbf{C}_{yr} \hat{\mathbf{x}}_r - \mathbf{D}_{yr} u) \quad (29)$$

$$\mathbf{L} = [\tilde{\mathbf{R}}^{-1}(\gamma \mathbf{F}_{yr} \mathbf{E}_r' + \mathbf{C}_{yr} \mathbf{S})]' \quad (30)$$

where  $\mathbf{S}$  is the solution of the algebraic Riccati equation given by

$$\mathbf{0} = \mathbf{S} \tilde{\mathbf{A}} + \tilde{\mathbf{A}}' \mathbf{S} - \mathbf{S} \tilde{\mathbf{G}} \mathbf{S} + \tilde{\mathbf{H}} \quad (31)$$

and

$$\tilde{\mathbf{A}} = \mathbf{A}_r' - \mathbf{C}_{yr}' \tilde{\mathbf{R}}^{-1}(\gamma \mathbf{F}_{yr} \mathbf{E}_r') \quad (32)$$

$$\tilde{\mathbf{G}} = \mathbf{C}_{yr}' \tilde{\mathbf{R}}^{-1} \mathbf{C}_{yr} \quad (33)$$

$$\tilde{\mathbf{H}} = \gamma \mathbf{E}_r \mathbf{E}_r' - \gamma^2 \mathbf{E}_r \mathbf{F}_{yr}' \tilde{\mathbf{R}}^{-1} \mathbf{F}_{yr} \mathbf{E}_r' \quad (34)$$

$$\tilde{\mathbf{R}} = \mathbf{I} + \gamma \mathbf{F}_{yr} \mathbf{F}_{yr}' \quad (35)$$

Calculations to determine  $\mathbf{L}$  were done using the MATLAB routine *lqew.m* within the control toolbox.

Finally, the controller is put in the form of Eqs. (4–5) using the bilinear transformation (Antoniu, 1993) to yield the following compensator

$$\mathbf{x}_{k+1}^c = \mathbf{A}^c \mathbf{x}_k^c + \mathbf{B}^c \mathbf{y}_k \quad (36)$$

$$u_k = \mathbf{C}^c \mathbf{x}_k^c + \mathbf{D}^c \mathbf{y}_k \quad (37)$$

As required, the  $\dim(\mathbf{x}_k^c) = 10 \leq 12$ .

To assess the performance of the sample controller, it is implemented on the evaluation model discussed previously. Based on an eigenvalue analysis, both the controller and the closed-loop system are stable. The loop gain transfer function was used to provide an indication of the closed-loop stability of the system. Here, the loop gain transfer function is defined as the transfer function of the system formed by breaking the control loop at the input to the system (Dyke, *et al.*, 1994b, 1996a,b). The loop gain formed with this control design is provided in Fig. 6. A control design was considered to be robust if the magnitude of the loop gain was below  $-5$  dB at all frequencies above 35 Hz.

For the first five evaluation criteria, the rms values of the constraint variables are  $\sigma_{x_m} = 0.671$  cm,  $\sigma_{\ddot{x}_{am}} = 1.12$  g and  $\sigma_u = 0.143$  V. For evaluation criteria six through ten, the peak values of the constraint variables are  $x_m = 2.00$  cm,  $\ddot{x}_{am} = 4.83$  g and  $u = 0.526$  V. Thus, all control design constraints were achieved with this control design. The associated evaluation

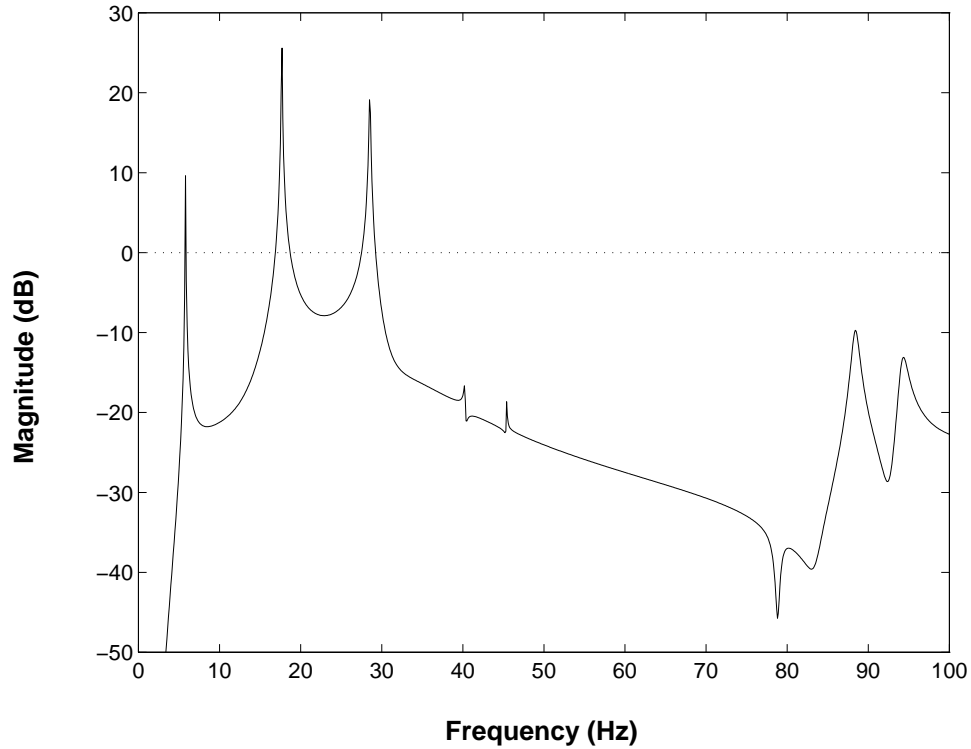


**Figure 6. Loop Gain Transfer Function for Sample Control Design.**

**Table 1: Evaluation Criteria for the Sample Controller.**

$J_1$	0.283	$J_6$	0.456
$J_2$	0.440	$J_7$	0.681
$J_3$	0.510	$J_8$	0.669
$J_4$	0.513	$J_9$	0.771
$J_5$	0.628	$J_{10}$	1.28

criteria are given in Table 1. Note that the rms and peak responses were determined through simulation using the SIMULINK program shown in Figure 5. The rms responses were calculated assuming an ergodic response and averaging over a 300 second time period.

## CLOSURE

The 28-state evaluation model, as well as the 10-state control design model, the MATLAB (1994) m-file used to do the sample control design, the input data and the simulation model are available on the World Wide Web at the following URL:

<http://www.nd.edu/~quake/>

Additionally, all control designs reported in this special issue of the Journal are available at this URL. If you cannot access the World Wide Web or have questions regarding the benchmark problem, please contact the senior author via e-mail at: [spencer.1@nd.edu](mailto:spencer.1@nd.edu).

## ACKNOWLEDGMENTS

This research is partially supported by National Science Foundation Grant Nos. CMS 95–00301 and CMS 95–28083 (Dr. S.C. Liu, Program Director). The input provided by the Committee on Structural Control, ASCE Structural Division is also acknowledged. The assistance of Dr. Erik A. Johnson in editing, evaluating the control designs, and preparing the Web site results is gratefully appreciated.

## APPENDIX I – REFERENCES

- Antoniou, A. (1993). *Digital Filters: Analysis, Design, and Applications*, McGraw-Hill, Inc., New York, pp. 444–446.
- Chung, L.L., Lin, R.C., Soong, T.T. and Reinhorn, A.M. 1989. Experiments on Active Control for MDOF Seismic Structures,” *J. of Engrg. Mech.*, ASCE, Vol. 115, No. 8, pp. 1609–27.
- Dyke, S.J., Spencer Jr., B.F., Belknap, A.E., Ferrell, K.J., Quast, P., and Sain, M.K. (1994a). “Absolute Acceleration Feedback Control Strategies for the Active Mass Driver.” *Proc. First World Conference on Structural Control*, Pasadena, California, August 3–5, 1994, Vol. 2, pp. TP1:51–TP1:60.
- Dyke, S.J., Spencer Jr., B.F., Quast, P., Sain, M.K., Kaspari Jr., D.C. and Soong, T.T. (1994b). “Experimental Verification of Acceleration Feedback Control Strategies for An Active Tendon System,” *National Center for Earthquake Engineering Research Technical Report NCEER–94–0024*, August 29.
- Dyke, S.J., Spencer Jr., B.F., Quast, P., Kaspari Jr., D.C. and Sain, M.K. (1996a). “Implementation of an Active Mass Driver Using Acceleration Feedback Control.” *Microcomputers in Civil Engrg.*, Vol. 11, pp. 305–323.
- Dyke, S.J., Spencer Jr., B.F., Quast, P., Sain, M.K., Kaspari Jr., D.C. and Soong, T.T. (1996b). “Acceleration Feedback Control of MDOF Structures.” *J. Engrg. Mech.*, ASCE, Vol. 122, No. 9, pp. 907–918.
- Fujino, Y., Soong, T.T. and Spencer Jr., B.F. (1996). “Structural Control: Basic Concepts and Applications.” *Proceedings of the ASCE Structures Congress XIV*, Chicago, Illinois, pp. 1277–1287.
- Housner, G.W., Masri, S.F., and Chassiakos, A.G., Eds. (1994a). *Proceedings of the First World Conference on Structural Control*, International Association for Structural Control, Los Angeles.
- Housner, G.W., Soong, T.T. and Masri, S. (1994b). “Second Generation of Active Structural Control in Civil Engineering.” *Proc. First World Conference on Structural Control*, Pasadena, California, August 3–5, 1994, Vol. 1, pp. Panel:3–18.
- Ivers, D.E. and Miller, L.R. (1991). “Semi-Active Suspension Technology: An Evolutionary View.” *DE-Vol. 40, Advanced Automotive Technologies*, (S.A. Velinsky, R.H. Fries and D. Wang, Eds.), ASME Book No. H00719, pp. 327–346.
- MATLAB (1994). The Math Works, Inc. Natick, Massachusetts.
- Quast, P., Sain, M.K., Spencer Jr., B.F. and Dyke, S.J. (1995). “Microcomputer Implementations of Digital Control Strategies for Structural Response Reduction,” *Microcomputers in Civil Engrg.*, Vol. 10, pp. 13–25.
- SIMULINK (1994). The Math Works, Inc. Natick, Massachusetts.

- Skelton, R.E. (1988). *Dynamic Systems Control: Linear Systems Analysis and Synthesis*. Wiley, New York.
- Soong, T.T. *Active Structural Control: Theory and Practice*, Longman Scientific and Technical, Essex, England, 1990.
- Stengel, R.F. (1986). *Stochastic Optimal Control: Theory and Application*. Wiley, New York.
- Yao, J.T.P. (1972). "Concept of Structural Control." *ASCE J. Struct. Div.*, Vol. 98, pp. 1567–1574.

## APPENDIX II – NOMENCLATURE

- A, B, E**
- C<sub>y</sub>, D<sub>y</sub>, F<sub>y</sub>** – state space matrices for the evaluation model
- C<sub>z</sub>, D<sub>z</sub>, F<sub>z</sub>**
- A<sub>r</sub>, B<sub>r</sub>, E<sub>r</sub>** – state space matrices for the reduced order model
- C<sub>yr</sub>, D<sub>yr</sub>, F<sub>yr</sub>**
- A<sup>c</sup>, B<sup>c</sup>** – state space matrices for the discrete controller
- C<sup>c</sup>, D<sup>c</sup>**
- d<sub>i</sub>** – interstory drift of the *i*th floor
- f<sub>1</sub>(·), f<sub>2</sub>(·)** – feedback compensator functions
- H<sub>ẍẍ</sub>(s)** – transfer function of the filters used to obtain the pseudo absolute velocities
- J** – performance function for LQG control design
- J<sub>i</sub>** – *i*th evaluation criteria
- K** – full state feedback gain matrix
- k** – discrete time step index
- L** – state estimator gain matrix
- P** – algebraic Riccati matrix solution for regulator
- Q, r** – weights in LQG control design
- S** – algebraic Riccati matrix solution for state estimator
- S<sub>v<sub>i</sub>v<sub>i</sub></sub>** – magnitude of the constant two-sided spectral density for the white noises modeling the measurement noise in the LQG control design
- S<sub>ẍ<sub>g</sub>ẍ<sub>g</sub></sub>** – magnitude of the constant two-sided spectral density for the white noise used to model the ground excitation in the LQG control design
- T** – sampling time
- u** – scalar control input
- u<sub>k</sub>** – scalar control input at time  $t = kT$
- v** – measurement noise vector for the evaluation model
- v<sub>r</sub>** – measurement noise vector for the control design model
- x** – state vector for the evaluation model
- x<sub>k</sub><sup>c</sup>** – state vector for the discrete controller at time  $t = kT$
- x<sub>r</sub>** – state vector for the control design model
- ẋ<sub>r</sub>** – estimated state vector for the control design model
- x<sub>i</sub>** – displacement of the *i*th floor relative to the ground
- x<sub>m</sub>** – displacement of the actuator piston relative to the third floor

- $x_{3o}$  – peak third floor displacement response relative to the ground of the uncontrolled building for each respective historical earthquake
- $\dot{x}_i$  – velocity of the  $i$ th floor relative to the ground
- $\dot{x}_{3o}$  – peak third floor velocity response relative to the ground of the uncontrolled building for each respective historical earthquake
- $\dot{\tilde{x}}_{ai}$  – pseudo absolute velocity of the  $i$ th floor
- $\dot{x}_m$  – velocity of the actuator piston relative to the third floor
- $\dot{\tilde{x}}_{am}$  – pseudo absolute velocity of the actuator piston
- $\dot{\tilde{x}}_g$  – pseudo absolute velocity of the ground
- $\ddot{x}_{ai}$  – absolute acceleration of the  $i$ th floor
- $\ddot{x}_{am}$  – absolute acceleration of the actuator piston
- $\ddot{x}_g$  – absolute acceleration of the ground
- $\ddot{x}_{a3o}$  – peak third floor absolute acceleration of the uncontrolled building for each respective historical earthquake
- $\mathbf{y}$  – vector of directly measured responses
- $\mathbf{y}_k$  – vector of directly measured responses sampled at time  $t = kT$
- $\mathbf{y}_r$  – output vector for the control design model
- $\tilde{\mathbf{y}}$  – vector of responses available for calculation of the control
- $\tilde{\mathbf{y}}_k$  – vector of responses available for calculation of the control sampled at time  $t = kT$
- $\mathbf{z}$  – vector of regulated responses
- $\sigma_{d_i}$  – rms interstory drift of the  $i$ th floor
- $\sigma_u$  – rms control signal
- $\sigma_{x_m}$  – rms displacement of the actuator piston relative to the third floor
- $\sigma_{\ddot{x}_g}$  – rms ground acceleration
- $\sigma_{x_{3o}}$  – worst-case stationary rms displacement of the third floor of the uncontrolled building relative to the ground
- $\sigma_{\dot{x}_m}$  – rms velocity of the actuator piston relative to the third floor
- $\sigma_{\dot{x}_{3o}}$  – worst-case stationary rms velocity of the third floor of the uncontrolled building relative to the ground
- $\sigma_{\ddot{x}_{a3o}}$  – worst-case stationary rms absolute acceleration of the third floor of the uncontrolled building
- $\sigma_{\ddot{x}_{ai}}$  – rms absolute acceleration of the  $i$ th floor
- $\omega_g, \zeta_g$  – parameters of the Kanai–Tajimi spectrum